Torque Control Scheme for PMSM in Overmodulation Range

Smith Lerdudomsak Shinji Doki Shigeru Okuma
Department of Electrical Engineering and Computer Science
Nagoya University
Nagoya, Japan
Phone: +81 (52) 789-2777
Fax: +81 (52) 789-3140
Email: smith@okuma.nuee.nagoya-u.ac.jp,doki@nagoya-u.jp,okuma@nagoya-u.jp
URL: http://www.okuma.nuee.nagoya-u.ac.jp

Keywords

<<PMSM>>, <<Overmodulation>>, <<Torque Control>>

Abstract

In this paper, torque control scheme for PMSM when an inverter operates in the overmodulation range is proposed and examined. The torque control system has our proposed closed-loop current control system, which harmonic current compensation scheme is used to improve the stability in the overmodulation range. Finally, the overall torque control performance will be evaluated by the experimental results.

Introduction

For expanding the operating range of permanent magnet synchronous motors (PMSMs), there are many efforts to utilize an inverter in the overmodulation range. However, because of the effect from harmonic currents generated in this range, a closed loop current control system may become unstable [1][7]. For solving this instability problem, many harmonic current compensation schemes were proposed (also by the authors too)[1]-[6].

However, the performance of the overall torque control system is still not examined well. In this paper, the torque control system, which has our proposed closed-loop current control system with harmonic current compensation is proposed. The performance of the torque control system is examined and evaluated over the entire torque-speed range, when an inverter operates from the linear range to the overmodulation range.

Closed loop current control system with harmonic current compensation

The structure of our proposed current control system is shown in Fig.1. Compared with the conventional current control system, an amplitude compensator and harmonic current estimator are added. An amplitude compensator is a table contained the inverter input-output voltage amplitude relation, and is used to compensate the nonlinearity of an inverter in the overmodulation range [8].

As stated before, harmonic current compensation scheme is used to improve stability in the overmodulation range, thus an harmonic current estimator is necessary. The details of harmonic current estimation method that proposed by the authors[5] can be summarized as below.

First, for estimating the harmonic voltages by using only the reference voltages information, an inverter model is necessary. In this time, we pay an attention on the conventional and simple Sine-PWM modulation method, however an inverter model that propose here can also be applied to the other modulation methods too.

In Sine-PWM modulation method, waveforms of u-phase inverter reference voltages and output voltage are shown together in Fig.2(a), when V_u^{**} is u-phase reference voltage calculated from current controllers (after voltage limiter calculation), V_u^{***} is reference voltage after amplitude compensation and V_u is inverter output voltage respectively. If the reference voltage V_u^{***} is limitted by $\pm V_{DC}/2$ limiter,

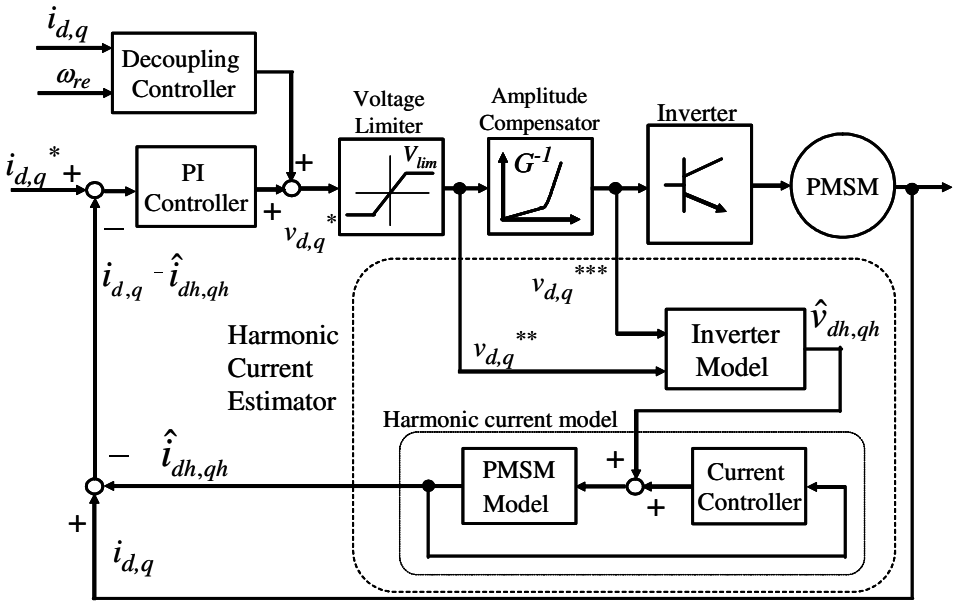

Figure 1: Closed loop current control system with harmonic current compensation

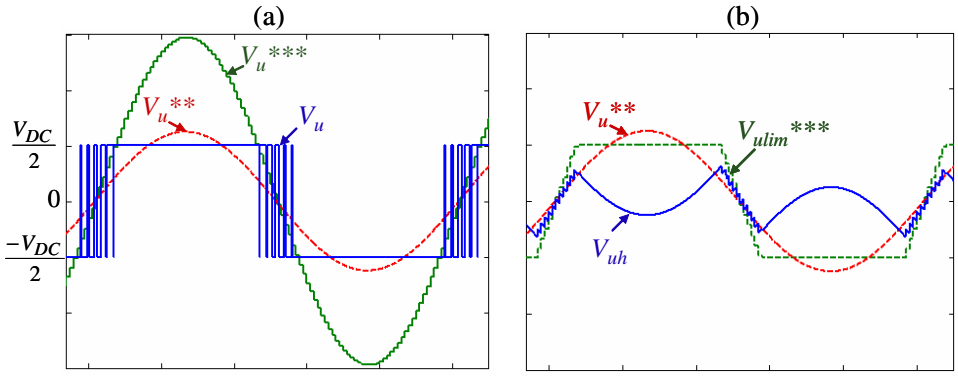

Figure 2: Waveform of inverter reference and output voltage in overmodulation range

it becomes V_{ulim}^{***} as showm in Fig2(b). This V_{ulim}^{***} contains both fundamental and harmonic components information of the output voltage V_u.

Hence,the u-phase harmonic voltage $\hat{V}_{uh}$ can be estimated as shown in (1) by the difference between V_{ulim}^{***} and reference voltage V_u^{**} (that represents fundamental component of inverter output voltage). The harmonic voltages in v-phase and w-phase $\hat{V}_{vh}$,$\hat{V}_{wh}$ can also be estimated by the same method. Then, the harmonic voltages in d-q axis rotational frame $\hat{v}_{dh}$,$\hat{v}_{qh}$ can be obtained by using the conventional Park transformation with harmonic voltages in three phases system.

$$\hat{V}_{uh} = V_{ulim}^{***} - V_u^{**} \tag{1}$$

Next, the state equations of harmonic current model used in harmonic current estimator can be shown in (2). This model is the state equations of the closed loop system that composed of a PMSM and d-q axis PI current controllers. The difference between the model proposed by the authors and the other harmonic current models is that, the effect from PI current controller is also considered here, thus the stability of current control system can be attained even in transient condition [5].

$$\begin{bmatrix} \dot{\hat{i}}_{dh} \\ \dot{\hat{i}}_{qh} \\ \dot{\hat{e}}_{dh} \\ \dot{\hat{e}}_{qh} \end{bmatrix} = \begin{bmatrix} -\left(\frac{R+K_{pd}}{L_d}\right) & 0 & \frac{K_{id}}{L_d} & 0 \\ 0 & -\left(\frac{R+K_{pq}}{L_q}\right) & 0 & \frac{K_{iq}}{L_q} \\ -1 & 0 & 0 & 0 \\ 0 & -1 & 0 & 0 \end{bmatrix} \begin{bmatrix} \hat{i}_{dh} \\ \hat{i}_{qh} \\ \hat{e}_{dh} \\ \hat{e}_{qh} \end{bmatrix} + \begin{bmatrix} \frac{1}{L_d} & 0 \\ 0 & \frac{1}{L_q} \\ 0 & 0 \\ 0 & 0 \end{bmatrix} \begin{bmatrix} \hat{v}_{dh} \\ \hat{v}_{qh} \end{bmatrix} \tag{2}$$

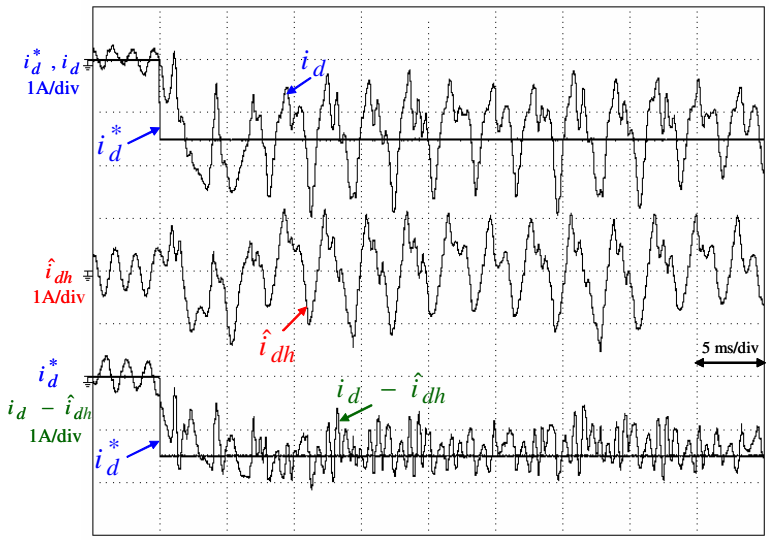

Figure 3: Estimated result of d-axis harmonic current

In (2), $[\hat{i}_{dh} \ \ \hat{i}_{qh}]^T$ are estimated d and q axis harmonic currents, $[\hat{v}_{dh} \ \ \hat{v}_{qh}]^T$ are estimated d and q axis inverter harmonic voltages (from inverter model in Fig.1 as stated before), $[\hat{e}_{dh} \ \ \hat{e}_{qh}]^T$ are estimated integration values of d and q axis harmonic current errors, $K_{pd}, K_{pq}, K_{id}, K_{iq}$ are d and q axis proportional and integral gains of current controllers respectively. Parameters of PMSM used in this model are L_d, L_q, R which represent values of d and q axis inductances and resistance respectively.

An example of the experimental result of estimated d-axis current by the proposed method is shown in Fig.3, when $i_d^*, i_d, \hat{i}_{dh}, i_d - \hat{i}_{dh}$ are d-axis reference current, d-axis real current, estimated d-axis harmonic current and d-axis current after harmonic compensation respectively. From this result, we can find that, with the proposed method, the harmonic current can be correctly estimated even in transient condition.

Opened loop torque controller

The structure of torque controller used in this paper is shown in Fig.4, which consists of torque-speed limiter table, maximum torque/current control table and flux weakening control table. This structure is same as the other conventional opened loop torque controllers [9], however, the maximum of inverter output voltage ,used in the calculation of these tables, is the value when an inverter operates in the overmodulation range at six step operation and can be shown in (3), when V_{dc} represents DC link voltage. Our proposed stable closed-loop current control scheme described in the previous section, makes it is possible to operate torque control even in the overmodulation range.

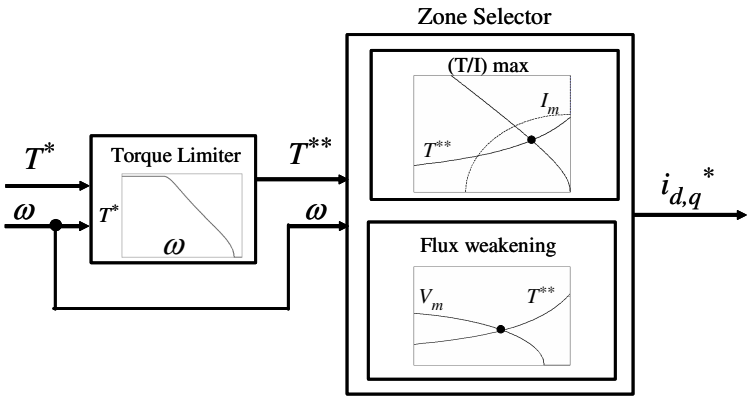

Figure 4: Structure of opened loop torque controller

$$V_{lim} = \sqrt{\frac{3}{2}}\frac{4}{\pi}\frac{V_{DC}}{2} \tag{3}$$

In this paper, the setting values of the DC link voltage and maximum current are shown in TABLE I and the parameters of PMSM are shown in TABLE II. With these parameters, the maximum torque-speed curve in the linear and the overmodulation range can be plotted together as shown in Fig.5. In this paper, the maximum torque control along the solid line (overmodulation range) in Fig.5 will be examined.

Table I: Setting parameters

DC link voltage	60 V
Maximum current	5 A
PI-Gain of current controllers	2000rad/s and 4000rad/s
Current control period	100μsec
Inverter carrier frequency f_c	10kHz
Voltage limiter calculation	Constant d-axis voltage
Antiwindup calculation	Back propagation

Table II: PMSM parameters

pole pairs P	2
EMF constant k_e	0.104V/(rad/s)
Resistance R	0.45Ω
d-axis inductance L_d	4.15mH
q-axis inductance L_q	16.74mH

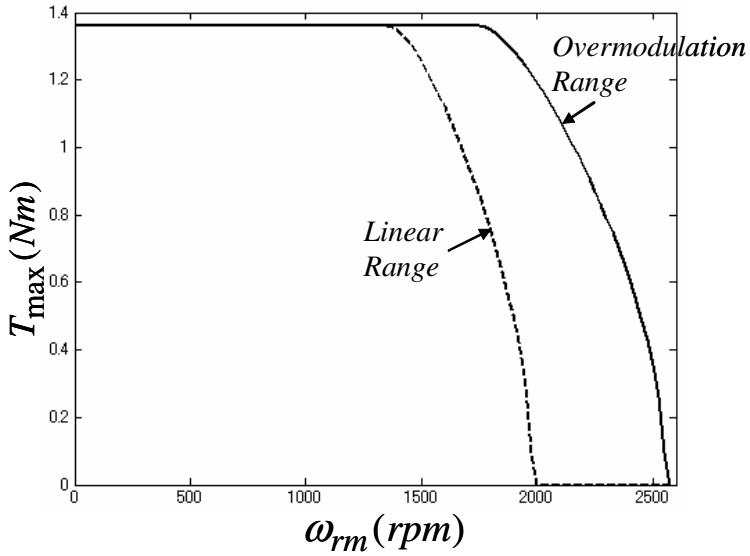

Figure 5: Maximum torque-speed curve

Experimental Results

Setting parameters of current control system and parameters of PMSM used in the experiment are shown in TABLE I and TABLE II respectively. The rotational speed of tested motor is changed from 0 rpm → 2500 rpm → 0 rpm in ramp by the other load motor. Reference torque is changed corresponding to the rotational speed along the solid line in Fig.5 which is the maximum torque that PMSM can generate under the limitation of current and voltage shown in TABLE I.

The corresponding reference d-q axis currents are calculated form torque controller shown in Fig.4. Crossover frequency of current controller PI gains that considered here are 2,000 rad/s and 4,000 rad/s. The performance when harmonic current compensation scheme is and is not used will be examined together.

The experimental results which are rotational speed (ω: rpm), reference voltage amplitude before voltage limiter (V^*: volt), limit of reference voltage amplitude at six step operation (V_{lim} : volt), reference torque (T^* : Nm), PMSM output torque which calculated from currents and PMSM parameters (T : Nm), d-q axis reference currents (i_d^*, i_q^*: A) and d-q axis real currents (i_d, i_q: A) will be shown together.

(1) The experimental results when PI gain = 2,000 rad/s, with and without harmonic current compensation scheme are shown in Fig.6 and Fig.7 respectively. From Fig.6, we can find that torque can be stably controlled even in the overmodulation range. However, due to the effect from harmonic currents, compared with the reference torque, torque error occurs. Therefore, in Fig.7, when harmonic current compensation scheme is used, this torque error is eliminated and torque can be correctly controlled.

(2) The experimental results when PI gain = 4,000 rad/s, with and without harmonic current compensation scheme are shown in Fig.8 and Fig.9 respectively. From Fig.8, we can find that when PI gain is large, torque control and current control become unstable in the overmodulation range due to harmonic currents as stated before. Therefore, in Fig.9, when harmonic current compensation scheme is used, torque and current can be stably and correctly controlled even in the overmodulation range and high gain condition.

Moreover, the result of inverter output voltage in stationary frame when rotational speed is 2,000 rpm is shown in Fig.10. From this result, we can find that the shape of output voltage is hexagon, hence an inverter is fully utilized.

(3) The experimental results when PI gain = 4,000 rad/s, with harmonic current compensation scheme and reference torque is changed in step form 100% $\rightarrow$ 10% and 10% $\rightarrow$ 100% when rotational speed is 1,700 rpm and 1,900 rpm is shown in Fig.11, which we can find that torque can be stably and correctly controlled even in transient condition and this is the main advantage of our proposed harmonic current estimation scheme as stated before.

Conclusions

In this paper, torque control scheme of a PMSM in the overmodulation range is considered and investigated. Based on the harmonic current estimation scheme that was proposed by the authors, a conventional torque control scheme in the linear range can be expanded to the overmodulation range. Many experimental results show the stability of the torque control system from the linear range to the overmodulation range of an inverter, over the entire torque-speed range of a PMSM (constant torque range and flux weakening range), and both in steady state and transient condition.

References

[1] A.M.Khambadkone and J.Holtz "Compensated Synchronous PI Current Controller in Overmodulation Range and Six-Step Operation of Space-Vector-Modulation-Based Vector-Controlled Drives" *IEEE Trans. Industrial Electronics*, vol. 49,no.3,June. 2002 pp. 574–580.

[2] H.W.Kim,N.V Nho and M.J.Youn "Current Control of PM Synchronous Motor in Overmodulation Range," *Proc.of the IECON 2004*, pp. 896-901.

[3] G.Dong and O.Ojo "A Generalized Over-modulation Methodology for Current Regulated Three-phase Voltage Source Converters" *Proc.of the IAS 2004*, pp. 2216–2223.

[4] S.Lerdudomsak, M.Kadota, S.Doki and S.Okuma "Harmonic Currents Estimation and Compensation Method for Current Control System of IPMSM in Overmodulation Range," *Proc.of the PCC-Nagoya 2007* , pp. 1320-1326.

[5] S.Lerdudomsak, S.Doki and S.Okuma "A Novel Current Control System for PMSM Considering Effects from Inverter in Overmodulation Range," *Proc.of the PEDS 2007* , pp. 794-800.

[6] S.Lerdudomsak, S.Doki and S.Okuma "Harmonic Currents Estimation and Compensation for Current Control System of PMSM in Overmodulation Range - Analysis for Robustness to Parameter Variations," *Proc.of the 2008 IECON Conf.*,pp. 1216-1221.

[7] S.Lerdudomsak, S.Doki and S.Okuma "Analysis for Unstable Problem of PMSM Current Control System in Overmodulation Range" *Proc.of the 2008 IAS Conf.*

[8] A.H.Hava,R.J.Kerkman and T.A.Lipo "Carrier-Based PWM-VSI Overmodulation Strategies:Analysis, Comparison, and Design," *IEEE Trans. Power Electronics*, vol. 13,no.4,July 1998 pp. 674-689.

[9] S.Morimoto, M.Sanada, and Y.Takeda "Wide-speed Operation of Interior Permanent Magnet Synchronous Motors with High-performance Current Regulator " *IEEE Trans. Industrial Applications*, vol. 30,no.4,July/August 1994 pp. 920-926.

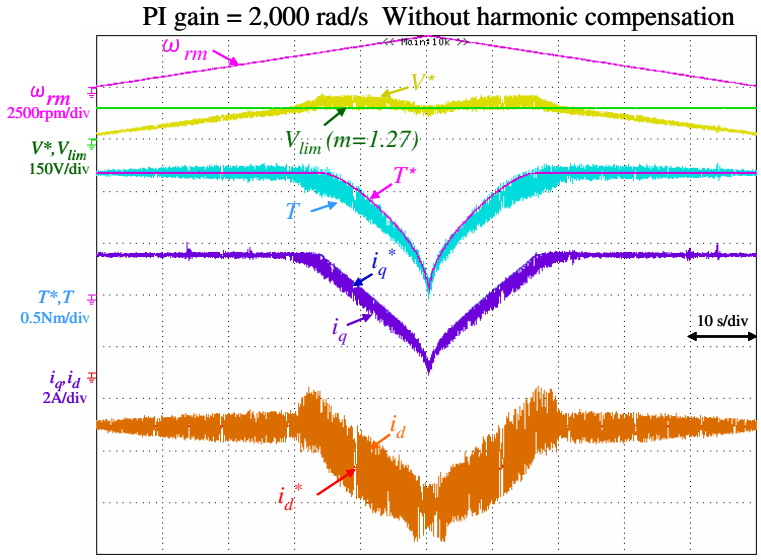

Figure 6: Experimental results: PI gain = 2,000 rad/s, without harmonic current compensation

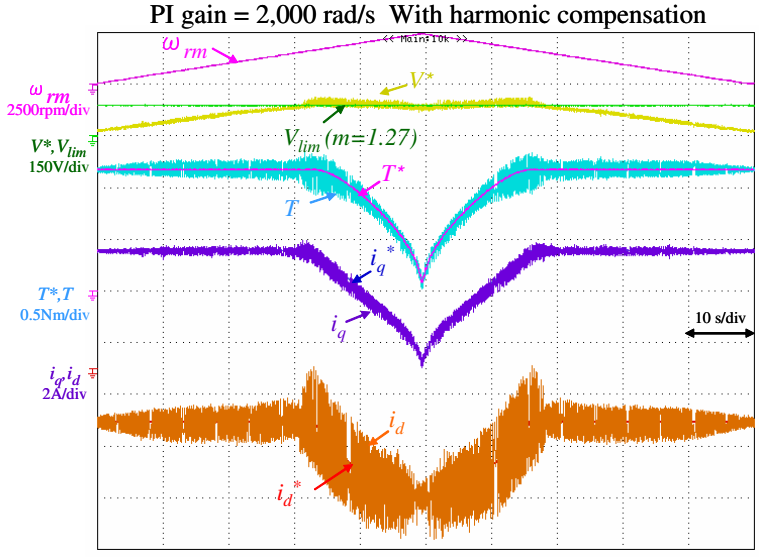

Figure 7: Experimental results: PI gain = 2,000 rad/s, with harmonic current compensation

 ISBN: 9789075815009

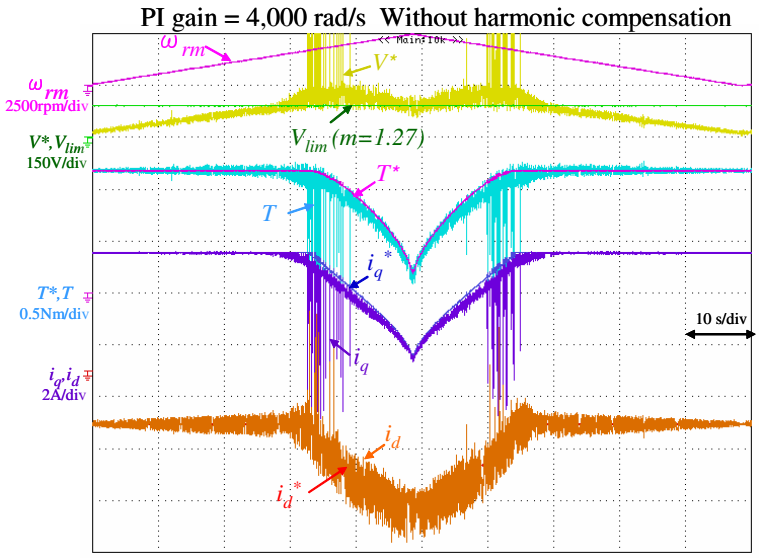

Figure 8: Experimental results: PI gain = 4,000 rad/s, without harmonic current compensation

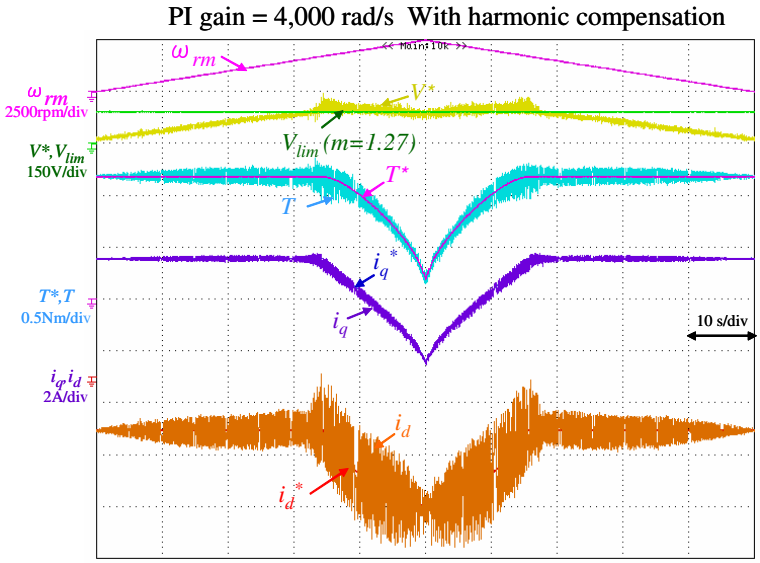

Figure 9: Experimental results: PI gain = 4,000 rad/s, with harmonic current compensation

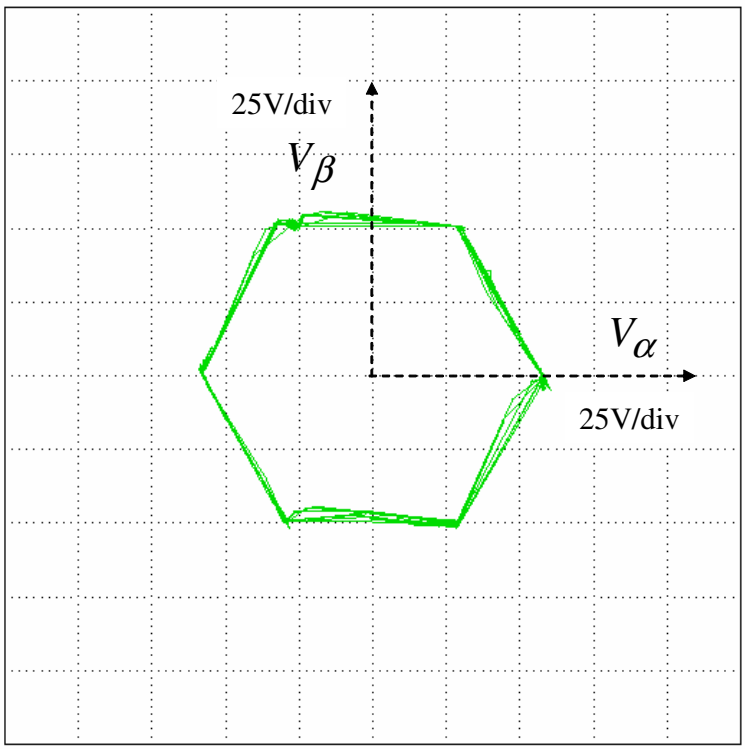

Figure 10: Experimental results: Inverter output voltage in stationary frame

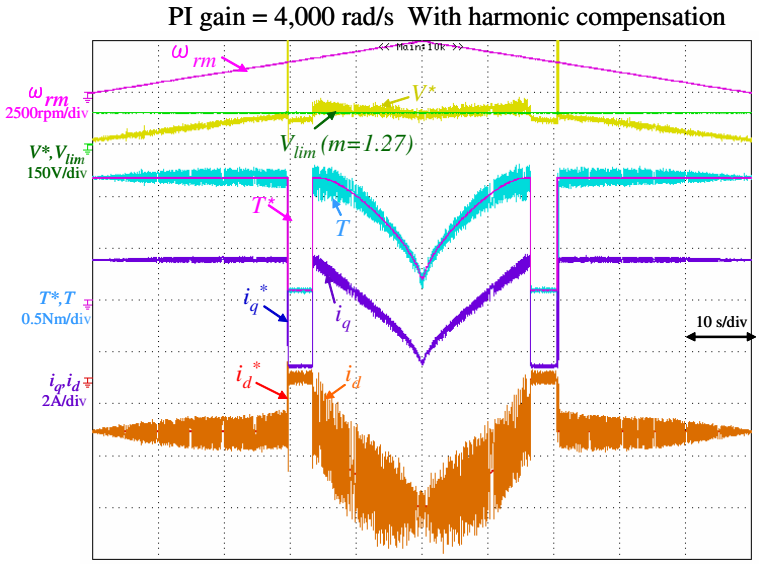

Figure 11: Experimental results: PI gain = 4,000 rad/s, with harmonic current compensation and step change in reference torque

 ISBN: 9789075815009